First principles determination of the model parameters in κ-$(ET)_2Cu_2(CN)_3$

Harald O. Jeschke[a], Hem C. Kandpal[b], Ingo Opahle[a], Yu-Zhong Zhang[a], Roser Valentí[a]

[a] *Institut für Theoretische Physik, Goethe-Universität Frankfurt, Max-von-Laue-Straße 1, 60438 Frankfurt am Main, Germany*
[b] *IFW Dresden, P.O. Box 270016, D-01171 Dresden, Germany*

Abstract

We present a detailed study of the derivation of the Hubbard model parameters for κ-$(ET)_2Cu_2(CN)_3$ in the framework of *ab initio* Density Functional Theory. We show that calculations with different (i) wavefunction basis, (ii) exchange correlation functionals and (iii) tight-binding models provide a reliable benchmark for the parameter values. We compare our results with available extended Hückel molecular orbital calculations and discuss its implications for the description of the properties of κ-$(ET)_2Cu_2(CN)_3$. The electronic properties of κ-$(ET)_2Cu(SCN)_2$ are also briefly discussed.

Key words:

1. Introduction

The search for possible candidates of a quantum spin liquid state has been one of the central issues in condensed matter physics since it was proposed several decades ago [1]. In the last years κ-$(ET)_2Cu_2(CN)_3$ has attracted much attention due to its unique realization of a pressure-induced Mott transition from a spin liquid state [2, 3, 4] to a metallic or even superconducting state at low temperatures.

A large amount of theoretical investigations on the one-band half-filled Hubbard model on the anisotropic triangular lattice have been carried out in order to understand the mechanism of the phase transition. Irrespective of the current debate on the phase diagram, such as presence or absence of spin-liquid or superconducting state, derived from this simplified model by various methods, like, path integral renormalization group approach [5], variational Monte Carlo method [6, 7], cluster extension of dynamical mean-field theory [8], or exact diagonalization [9] a question of fundamental importance is whether the existing model parameters obtained from extended Hückel molecular orbital calculations [10] are reliable or not, as they are the basis of all the mentioned theoretical work.

Recently we showed by full potential ab initio Density Functional Theory (DFT) calculations that the model parameters for κ-$(ET)_2Cu_2(CN)_3$ have to be qualitatively revised from t'/t=1.06 [10] to t'/t=0.83±0.08 [11], which casts doubts on the validity of the description of the system as coupled quasi-one-dimensional chains. Similar results were obtained by the authors of Ref. [12]. In the present paper, we discuss the importance of including in the results for t'/t the effects of considering different wavefunction bases as well as exchange correlation functionals within DFT. Furthermore, we show that alternative fitting procedures provide slightly different t'/t ratios. All these considerations lead to a statement of the t'/t ratios within a benchmark. Finally we also discuss the effects of longer ranged hoppings. These considerations are important for all κ-$(ET)_2X$ charge transfer salts and we present here also details of the bandstructure calculations and parameter determination for X=$Cu(SCN)_2$.

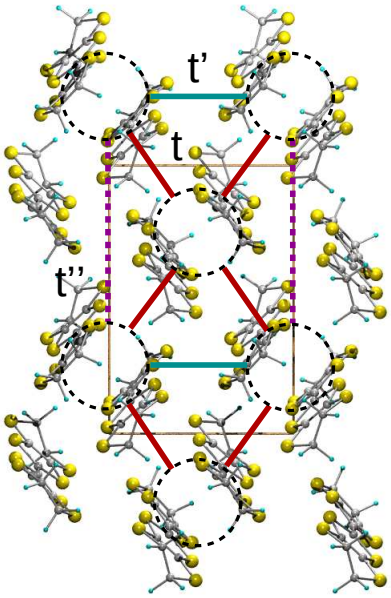

Figure 1: Structure of the κ BEDT-TTF arrangement for the example of κ-$(BEDT\text{-}TTF)_2X$ with X=$Cu_2(CN)_3$. t and t' form a frustrated triangular lattice.

2. Crystal structure and bandstructure calculations

The crystal structure of κ-$(ET)_2Cu_2(CN)_3$ consists of alternate stackings of pairs of ET = BEDT-TTF molecule donors (see Fig. 1) separated by $Cu_2(CN)_3$ acceptor layers. Each BEDT-TTF molecule consists of 10 carbon, 8 sulfur and 8 hydrogen atoms linked by covalent bonds. A common feature of κ-$(ET)_2Cu_2(CN)_3$ and other related BEDT-TTF based salts is the presence of conformational disorder. The two terminal ethylene groups in the BEDT-TTF molecule are twisted out of

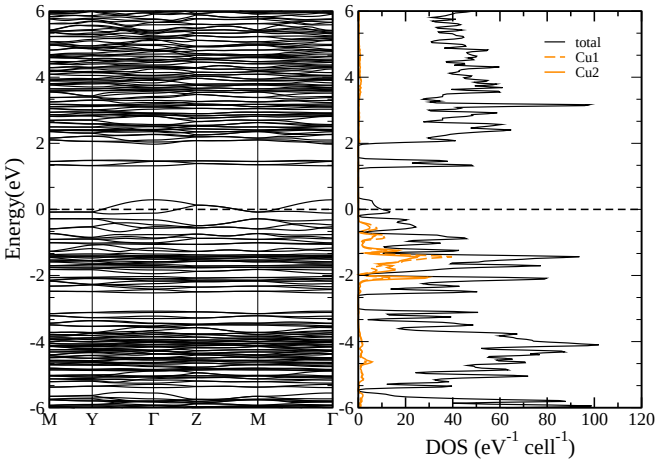

Figure 2: Band structure and density of states of κ-(BEDT-TTF)$_2$X with X=Cu$_2$(CN)$_3$, calculated with FPLAPW. The contribution of Cu to the DOS is highlighted. The Cu 3*d* states are fully occupied, indicating that Cu is in a nonmagnetic Cu^{+1} oxidation state.

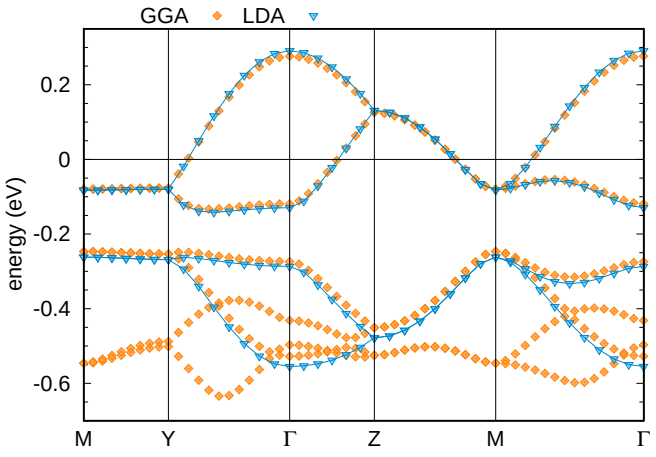

Figure 3: Comparison of low energy band structure between different exchange and correlation potentials for κ-(BEDT-TTF)$_2$X with X=Cu$_2$(CN)$_3$. The FPLO basis set was used. For GGA, two Cu 3*d* bands are entangled with the bonding bands of the BEDT-TTF dimer molecules; for LDA, they are clearly separate (starting below about -0.6 eV) and therefore not shown.

the molecular plane, and therefore this molecule has either an eclipsed or staggered conformation. The salt exhibits disorder at room temperature due to the random occurence of both conformations. The κ-(ET)$_2$Cu$_2$(CN)$_3$ salt crystallizes in the monoclinic space group $P2_1/c$. The inversion centre symmetry in $P2_1/c$ is guaranteed by the equal occupation of the two conformations. At low temperatures the staggered conformation dominates over the eclipsed conformation, therefore the staggered conformation was used in the calculations. The symmetry is then reduced to *Pc* with 120 atoms in the unit cell.

Moreover, since the hydrogen positions were not available from experiment [13] we introduced them in the structure and relaxed their positions by performing Car-Parrinello projector-augmented wave molecular dynamics (CPMD) calculations [14, 15, 16]. For these calculations we considered a (4 $\times$ 4 $\times$ 4) **k**-mesh in the Brillouin zone and plane wave cutoffs of 60 and 240 Ry for the wave function and the charge density, respectively.

The electronic structure was analyzed by considering two different all-electron codes, namely the the Full Potential Local Orbital method (FPLO version 8.50-32) [17, 18] and the Full Potential Linearized Augmented Plane Wave (FPLAPW) method as implemented in Wien2k [19]. We also performed comparative calculations with different exchange correlation functionals, the Local Density Approximation (LDA) in the parameterization of Perdew and Wang [20] and the Generalized Gradient Approximation (GGA) in the Perdew-Burke-Ernzerhof parameterization [21]. The convergency of the band structure with respect to the Brillouin zone integrations was checked with a series of calculations with up to 350 **k**-points in the full Brillouin zone. In the FPLAPW calculations a plane wave cut-off $R_{MT} \times k_{\max} = 3.37$ was used and the muffin-tin-radii for Cu, N, C, H, and S were chosen as 2.37, 1.06, 1.16/1.06, 0.92, and 2.00 a.u., respectively.

Despite the complexity of the crystal structure, the electronic structure of κ-(BEDT-TTF)$_2$Cu$_2$(CN)$_3$ in the vicinity of the Fermi energy is surprisingly simple. Fig. 2 shows the band structure and density of states for κ-(BEDT-TTF)$_2$Cu$_2$(CN)$_3$. Only two narrow, half filled bands with a width of about 0.4 eV cross the Fermi energy. Those bands are derived almost entirely from S 3p and C 2p states of the BEDT-TTF molecule and well separated from the remaining lower occupied and higher unoccupied bands. About 0.3 to 0.6 eV below the Fermi energy two further BEDT-TTF derived bands with mainly S 3p and C 2p character are visible. This is in an overall good agreement with the results of extended Hückel calculations [10], which find two anti-bonding bands of the highest occupied molecular orbital (HOMO) of the BEDT-TTF molecule intersecting the Fermi energy and place the corresponding bonding bands about 0.4 eV below the Fermi energy.

The Cu 3d states form a narrow band complex about 0.4 to 2.1 eV below the Fermi energy. The Cu 3d shell is completely filled, in agreement with the experimental reports [10] that the Cu atoms are in the Cu^{1+} state with 10 d electrons. A comparison of the band structure of κ-(ET)$_2$Cu$_2$(CN)$_3$ near the Fermi surface between the GGA and LDA functional is shown in Fig. 3. The two highest Cu 3d bands intersect the two bonding BEDT-TTF derived bands in GGA, whereas the LDA calculations place the Cu 3d bands further below the Fermi energy, so that the four BEDT-TTF derived bands near the Fermi energy are separated from the remaining bands within LDA. The difference in the position of the Cu 3d level between LDA and GGA amounts to about 0.2 eV, resulting in a rigid band shift with only a minute effect on the shape of the BEDT-TTF bands near the Fermi energy and the model parameters derived from them (see below). A similar difference between LDA and GGA derived band structures is also found in related κ-(BEDT-TTF)$_2$-X compounds [11]. There are also minor differences in the band structures calculated with the two different electronic structure codes (Fig. 4). While the two BEDT-TTF derived bands crossing the Fermi energy are almost exactly on top of each other, the lower occupied bands are shifted by about 50 meV between

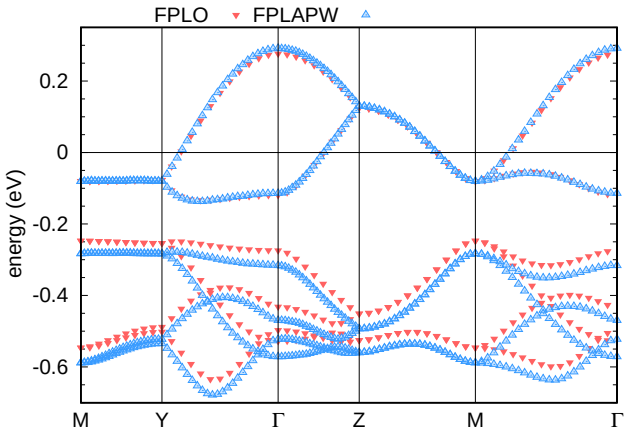

Figure 4: Comparison of low energy band structure between FPLAPW and FPLO basis sets for κ-(BEDT-TTF)$_2$X with X=Cu$_2$(CN)$_3$. The GGA exchange and correlation potential was used.

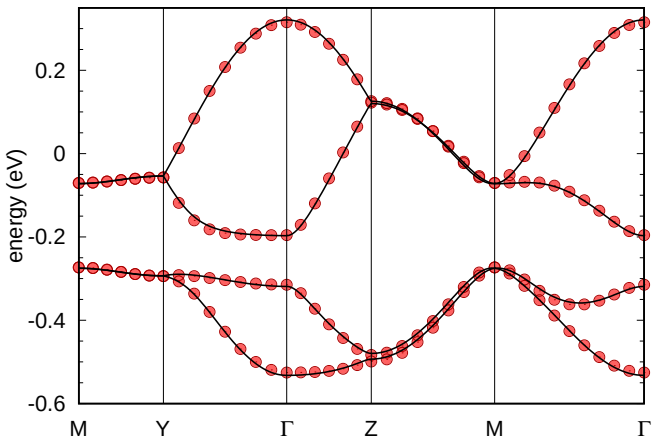

Figure 5: Low energy bandstructure of κ-(BEDT-TTF)$_2$X with X=Cu(SCN)$_2$ (symbols) and tight binding fit (lines). Note he lifting of the degeneracy at the Z point.

the FPLO and FPLAPW calculations. A possible reason for this difference could be the size of the basis set used in the calculations. However, we could not analyze the origin of these smaller differences in more detail, since the complexity of the crystal structure does not allow for extensive numerical checks.

In addition to the Cu 3d bands there are further BEDT-TTF derived bands in the energy region between -2.5 and -0.75 eV giving rise to the complex band structure shown in Fig. 2. Seperated by a pseudo gap of about 0.5 eV a complex manifold of BEDT-TTF and anion layer derived bands is visible starting from 3 eV below the Fermi energy. The higher unoccupied bands around 2 eV above the Fermi level have predominatly S 3p and C 2p character.

As comparison to the bandstructure of κ-(ET)$_2$Cu$_2$(CN)$_3$, we present in Fig. 5 the low energy bandstructure for κ-(ET)$_2$Cu(SCN)$_2$. While the overall features of the two bonding and antibondig bands are very similar to those of κ-(ET)$_2$Cu$_2$(CN)$_3$, κ-(ET)$_2$Cu(SCN)$_2$ shows a splitting of the bonding bands at the Z point which is not present in the bandstructure of κ-(ET)$_2$Cu$_2$(CN)$_3$.

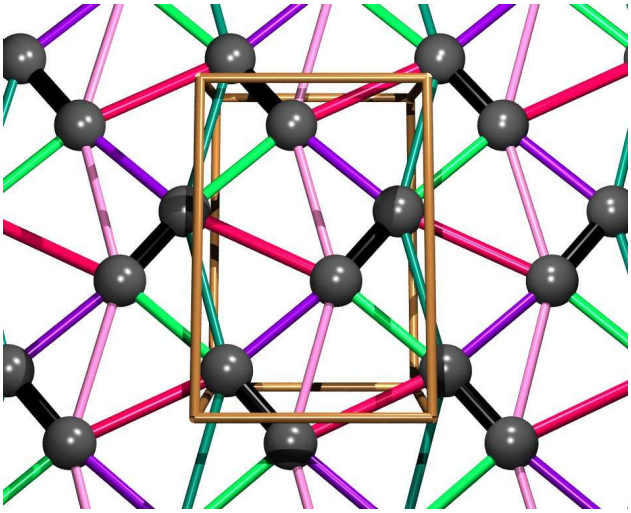

Figure 6: Lattice of BEDT-TTF molecules (grey spheres) for κ-(BEDT-TTF)$_2$X with X=Cu(SCN)$_2$. Dimer bonds (t_1) are shown in black, $t_4 \equiv t'$ in red. t has to be calculated from an average over t_2 (light green), t_3 (purple), t_5 (dark green) and t_6 (pink). The view is along the a direction, and the unit cell is marked.

The lifting of the degeneracy at Z is due to the slightly distorted arrangement of ET molecules in κ-(ET)$_2$Cu(SCN)$_2$ as shown in Fig. 6. This feature will also have implications on the determination of the tight-binding parameters as described below.

3. Model Hamiltonian

The half-filled Hubbard model

$$H = \sum_{<ij>,\sigma} t(c^\dagger_{i\sigma}c_{j\sigma} + \text{H.c.}) + \sum_{[ij],\sigma} t'(c^\dagger_{i\sigma}c_{j\sigma} + \text{H.c.}) + U\sum_i \left(n_{i\uparrow} - \frac{1}{2}\right)\left(n_{i\downarrow} - \frac{1}{2}\right).$$

on the triangular lattice has been proposed as the suitable Hamiltonian to describe the behavior of κ-(BEDT-TTF)$_2$Cu$_2$(CN)$_3$. t and t', as shown in Fig. 1 denote the hopping integrals between nearest neighbors $< i, j >$ and next nearest neighbors $[i, j]$ BEDT-TTF molecule dimers, respectively. Extensions of this Hamiltonian include also longer ranged hopping integrals, like t'', as well as nearest neighbor Coulomb integrals. In the following we shall concentrate on the calculation of the hopping matrix elements.

In order to obtain the hopping integrals t and t' out of the bandstructure calculations presented above, we have performed various tight-binding studies. One option, which we denote dimer model, consists of defining a BEDT-TTF dimer of molecules as a lattice site. The corresponding tight-binding model is then fitted to the two antibonding bands in Figs. 3 and 4, and the values of t, t', t'' and longer-ranged hopping parameters are directly obtained. The second option, or molecule model, considers the molecules in Fig. 1 as lattice sites and the corresponding tight-binding model is fitted to the four BEDT-TTF derived bands shown in Figs. 3 and 4. The parameters

t (meV)	t' (meV)	t'/t	method
Considering molecules as sites			
49	39	0.80	FPLO(GGA)
50	42	0.83	FPLAPW(GGA)
52	41	0.78	FPLO(LDA)
Considering dimers as sites			
50	45	0.90	FPLO(GGA)
52	47	0.91	FPLAPW(GGA)
53	47	0.88	FPLO(LDA)

Table 1: Hopping parameters t, t' and their ratio t/t' of κ-$(ET)_2Cu_2(CN)_3$ at ambient pressure, calculated with different basis sets (FPLO and FPLAPW) and functionals (LDA and GGA).

extracted from this calculation are hopping integrals between molecules. In order to relate the molecule-molecule hopping parameters with the dimer-dimer hopping parameters (t, t', t'') we consider the geometrical considerations given in Ref. [10]. This procedure was done for all bandstructure calculations discussed in the previous section. In Table 1 we present the results for t and t' with the various approaches.

While the differences between the sets of results are small, they are significant enough to be relevant for the determination of the t'/t ratio and define a margin of error of the DFT results. What is important about the results is that within the margin of error, the DFT calculations provide a clear prediction for the $t'/t < 1$ for κ-$(ET)_2Cu_2(CN)_3$ in disagreement with extended Hückel calculations that estimate $t'/t > 1$. Recent analysis of angular resolved magnetoresistance oscillations [22] predict a value of t'/t for κ-$(ET)_2Cu_2(CN)_3$ of ~ 0.93 in very good agreement with our results.

In the previous discussion we concentrated on the nearest and next nearest neighbor hopping integrals t, t'. It should be noted though that there are nonzero longer ranged hopping terms. In particular t'' in the dimer model has a value of 7 meV ($t''/t = 0.14$), which is nonnegligible.

In the tight-binding fit for κ-$(ET)_2Cu(SCN)_2$ the lifting of the degeneracy at the Z point can only be captured if the t_2, t_3 and t_5, t_6 of Fig. 6 are differentiated even though $t_2 \approx t_3$ and $t_5 \approx t_6$.

Finally we would like to note that while the half-filled Hubbard model on an anisotropic triangular lattice with t and t' hopping parameters is the minimal model that we can consider for the description of the system, a few extensions may be important like: (i) inclusion of longer ranged hopping terms, (ii) inclusion of longer ranged Coulomb interaction terms and (iii) consideration of the system at the level of molecules in terms of the quarter-filled Hubbard model [23].

4. Conclusions

In summary we have presented a detailed study of the derivation of Hubbard model parameters for κ-$(ET)_2Cu_2(CN)_3$ in the framework of Density Functional Theory. Comparison of the results obtained with different exchange and correlation functionals, high precision electronic structure codes as well as different tight binding models allows us to establish well defined bounds for the t'/t ratio used in model calculations. This analysis shows that the model parameters for κ-$(ET)_2Cu_2(CN)_3$ have to be qualitatively revised from t'/t=1.06 [10] to t'/t=0.83±0.08. Implications for the properties of κ-$(ET)_2Cu_2(CN)_3$ and possible extensions of the models are discussed.

5. Acknowledgements

We would like to thank M. Lang, J. Müller, F. Pratt and J. Merino for very useful discussions. We thank the Deutsche Forschungsgemeinschaft for financial support through the SFB/TRR 49 and Emmy Noether programs and we would like to acknowledge support by the Frankfurt Center for Scientific Computing.

References

[1] P. W. Anderson, Mater. Res. Soc. Bull. 8 (1973) 153.
[2] Y. Shimizu, K. Miyagawa, K. Kanoda, M. Maesato, G. Saito, Phys. Rev. Lett. 91 (2003) 1007001.
[3] S. Yamashita, Y. Nakazawa, M. Oguni, Y. Oshima, H. Nojiri, Y. Shimizu, K. Miyagawa, K. Kanoda Nature Physics 4 (2008) 459.
[4] M. Yamashita, N. Nakata, Y. Kasahara, T. Sasaki, N. Yoneyama, N. Kobayashi, S. Fujimoto, T. Shibauchi, Y. Matsuda Nature Physics 5 (2008) 44.
[5] T. Mizusaki, M. Imada Phys. Rev. B 74 (2006) 014421.
[6] T. Watanabe, H. Yokoyama, Y. Tanaka, J. Inoue, Phys. Rev. B 77 (2008) 214505.
[7] L. F. Tocchio, A. Parola, C. Gros, F. Becca, Phys. Rev. B 80 (2009) 064419.
[8] B. Kyung, A.-M. S. Tremblay, Phys. Rev. Lett. 97 (2006) 046402.
[9] R. T. Clay, H. Li, and S. Mazumdar, Phys. Rev. Lett. 101 (2008) 166403.
[10] T. Komatsu, N. Matsukawa, T. Inoue, G. Saito, J. Phys. Soc. Jpn. 65 (1996) 1340.
[11] H. C. Kandpal, I. Opahle, Y.-Z. Zhang, H. O. Jeschke, R. Valentí, Phys. Rev. Lett. 103 (2009) 067004.
[12] K. Nakamura, K. Nakamura, Y. Yoshimoto, T. Kosugi, R. Arita, M. Imada, J. Phys. Soc. Jpn. 78 (2009) 083710.
[13] U. Geiser, H. H. Wang, J. M. Williams, H. A. Charlier, J. E. Heindl, G. A. Yaconi, B. J. Love, M. W. Lathrop, J. E. Schirber, D. L. Overmyer, J. Ren, M.-H. Whangbo, Inorg. Chem. 30 (1991) 2586.
[14] R. Car and M. Parrinello, Phys. Rev. Lett. 55 (1985) 2471.
[15] M. Parrinello and A. Rahman, Phys. Rev. Lett. 45 (1980) 1196.
[16] P. E. Blöchl, Phys. Rev. B 50 (1994) 17953.
[17] K. Koepernik and H. Eschrig, Phys. Rev. B 59 1743 (1999); http://www.FPLO.de.
[18] I. Opahle, K. Koepernik, H. Eschrig, Phys. Rev. B 60 (1999) 14035.
[19] P. Blaha *et al.*, WIEN2K, An Augmented Plane Wave+Local Orbitals Program for Calculating Crystal Properties (Karlheinz Schwarz/Techn. Universität Wien, Wien, Austria, 2001).
[20] J. P. Perdew and Y. Wang, Phys. Rev. B 45 (1992) 13244.
[21] J. P. Perdew, K. Burke, and M. Ernzerhof, Phys. Rev. Lett. 77 (1996) 3865.
[22] Francis Pratt *private communication*.
[23] H. Li, R. T. Clay, S. Mazumdar, arXiv:0908.4109.